Adiabatic self-trapped states in zigzag nanotubes

2007 J. Phys.: Condens. Matter 19 306205

(http://iopscience.iop.org/0953-8984/19/30/306205)

IOP PUBLISHING JOURNAL OF PHYSICS: CONDENSED MATTER

J. Phys.: Condens. Matter **19** (2007) 306205 (22pp) doi:10.1088/0953-8984/19/30/306205

Adiabatic self-trapped states in zigzag nanotubes

L S Brizhik[1], A A Eremko[1], B M A G Piette[2] and W J Zakrzewski[2]

[1] Bogolyubov Institute for Theoretical Physics, 03680 Kyiv, Ukraine
[2] Department of Mathematical Sciences, University of Durham, Durham DH1 3LE, UK

E-mail: brizhik@bitp.kiev.ua, eremko@bitp.kiev.ua, B.M.A.G.Piette@durham.ac.uk and W.J.Zakrzewski@durham.ac.uk

Received 13 March 2007, in final form 16 May 2007
Published 11 July 2007
Online at stacks.iop.org/JPhysCM/19/306205

Abstract

We study the polaron (soliton) states of a quasiparticle (electron, hole, exciton) in a quasi-one-dimensional (quasi-1D) model which describes a carbon-type zigzag nanotube structure. In the Hamiltonian of the system we include the electron–phonon interaction that arises from the dependence of both the on-site and the hopping interaction energies on the lattice deformation. We derive, in the adiabatic approximation, the equations for the self-trapped states of a quasiparticle in a zigzag nanotube. We show that the ground state of such a system depends on the strength of the electron–phonon coupling and we find polaron-type solutions with different symmetries. Namely, at a relatively weak coupling a quasiparticle is self-trapped in a quasi-1D polaron state which has an azimuthal symmetry. When the coupling constant exceeds some critical value, the azimuthal symmetry breaks down and the quasiparticle state can be described as a two-dimensional small polaron on the nanotube surface. In the crossover region between the two solutions there is a range of intermediate couplings, in which the two structures, the quasi-1D polaron and the strongly localized 2D polaron, coexist as their energies are very close together. We note that the results of this analytical study are in quantitative agreement with what has recently been observed numerically.

1. Introduction

Many important physical properties of low-dimensional (LD) molecular systems are due to the electron–phonon interaction which can lead to the spontaneous breakdown of the translational symmetry of the system and to the formation of nonlinear states, such as self-trapped quasiparticles (electrons, holes or excitons), charge density waves, kinks, etc [1–4]. Studies, in one-dimensional (1D) (or quasi-1D) molecular systems, of self-trapped states of quasiparticles, i.e., of self-consistent states of a quasiparticle, and of the lattice distortion, have been attracting a great deal of interest for quite a while [4–6]. Various names have been

introduced for self-trapped electron states, such as polarons, condensons, fluctuons, solitons, etc. 'Polaron' is the most often used. This term was initially introduced by S I Pekar to describe a self-trapped state formed due to the interaction with the polarizational optical phonons in ion crystals. Since then, this term has been given a more general meaning and covers a wide class of self-trapped electron states such as 'acoustic polarons', 'optic Holstein polarons', 'piezo-polarons', etc. It has been shown that there are many real systems, including biological macromolecules, quasi-1D organic and inorganic compounds, and conducting polymers, in which self-trapping of quasiparticles takes place. The concept of solitons (1D polarons) has been used to explain various phenomena, such as charge and energy transports in α-helical proteins [4], in DNA [7], and in conducting polymers [8, 3, 9–11]. Recently a new class of 1D compounds, carbon [12–15] and boron nitride [16, 17] nanotubes, have been synthesized, and they have been intensively studied experimentally and theoretically ever since. These substances have found numerous practical applications, for instance, in miniaturized electronic, mechanical, electromechanical and optoelectronic devices. The possibility of the formation of states with a spontaneously broken symmetry in carbon nanotubes has been discussed in [18, 19]. In particular, large polarons in nanotubes have been considered in [20, 21]. Recently some experimental evidence of the existence of self-trapping in nanotubes has also been presented [22].

Usually, theoretical studies of such systems are based on a simplified model of an isolated chain with a single energy band. However, for the proper description of various properties of such systems one must take into account their complex structure, which is clearly more complicated than that of a chain with one atom per unit cell. In fact, this can result in the existence of various types of soliton, leading to the appearance of qualitatively new features, as, for instance, has been shown for α-helical proteins [23]. This is particularly true in the case of nanotubes whose properties can range from those of 1D metals to semiconductors depending on their diameters and chiralities [13, 14, 24, 18, 25]. The nanotubes possess series of energy bands which are determined by 1D energy dispersion relations dependent on the wavevector k along the nanotube axis. Thus, it is interesting to study the possibility of self-trapping of a quasiparticle in a system with the geometry of a carbon nanotube. A numerical study of the formation and properties of polaron states in zigzag nanotubes, in the semi-empirical tight-binding model with nearest-neighbours hopping interactions [13], has been reported in [26]. Here, we study this problem analytically and show that a quasiparticle in a zigzag nanotube can be self-trapped in various polaron-type states which possess different symmetries. We find that the quasiparticle ground state in such a system depends on the strength of the electron–phonon coupling. Namely, we show that at a relatively weak coupling polarons possess quasi-1D properties and have an azimuthal symmetry. When the coupling constant exceeds some critical value, the azimuthal symmetry is broken and the quasiparticle self-traps into a state of a small 2D polaron on the surface of the nanotube. There is also the crossover region in which the two types of polaron coexist and have very close energies.

2. Model of a nanotube

In this section we define the variables used to describe a nanotube. The geometry of a single-wall carbon nanotube (SWCNT) is based on a deformable 2D hexagonal lattice of a graphene sheet which is wrapped into a cylinder. The position of any carbon atom of a nanotube at its equilibrium can be described by the radius-vector

$$\vec{R}^0_{æ} = R(\vec{e}_x \sin\Theta_{æ} + \vec{e}_y \cos\Theta_{æ}) + \vec{e}_z z_{æ}, \tag{1}$$

where the index $æ = \{æ_1, æ_2, æ_3\}$ labels nanotube lattice sites, R is the radius of the nanotube, and the coordinates $\Theta_{æ}$ and $z_{æ}$ are the azimuthal angle and the position along the

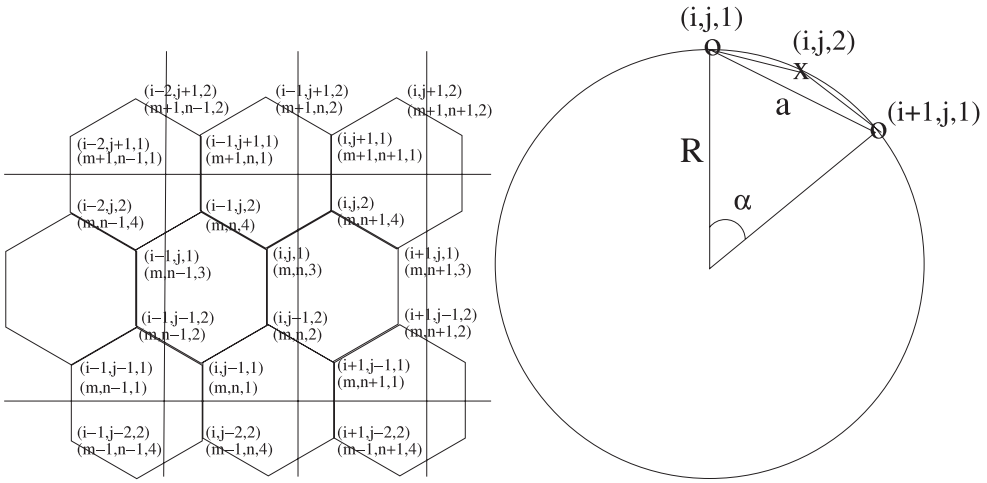

Figure 1. The two schemes of index labelling of a hexagonal lattice, and cross section of the nanotube.

tube, respectively. We consider zigzag nanotubes, as shown in figure 1, which represents the hexagonal lattice unfolded onto a plane and the horizontal cross section of the nanotube.

To label the sites of the nanotube, one can use two different schemes. The first one, the most commonly used, is based on the diatomic unit cell of the graphene sheet with nonorthogonal basic vectors. The corresponding labelling, $æ = \{i, j, \rho\}$, involves the indices $i = 0, \pm 1, \ldots$ and $j = 0, \pm 1, \ldots$ labelling shifts along the two basic vectors in the corresponding unrolled honeycomb lattice, and where the index $\rho = 1, 2$ labels the two types of atoms in a unit cell (usually called A and B): those who have the nearest neighbour one site 'down' ($\rho = 1$) and those who have it one site 'up' ($\rho = 2$)—see figure 1.

The second scheme is based on the translational vector which is defined to be the lattice vector of a 1D nanotube and which, together with the chiral vector, determines the rectangular unit cell for the nanotube [13]. Note that a zigzag hexagonal nanotube possesses two symmetries: the translation along the axis of the nanotube by the lattice constant (the modulus of the translational vector) and the rotation by an angle $\alpha = 2\pi/N$ around the nanotube axis. Here N is the number of hexagonal cells wrapped around a nanotube. Given this, one can use a labelling scheme in which the basic unit cell is rectangular and contains four atoms. For this scheme, also shown in figure 1, we use the labelling $æ = \{m, n, \varrho\}$, where $m = 0, \pm 1, \ldots$ is the axial index, $n = 1, 2, \ldots, N$ is the azimuthal index and $\varrho = 1, 2, 3, 4$ enumerates the atoms in the unit cell. The atoms with $\varrho = 1, 3$ have the nearest neighbour one site 'down', and those who have the nearest neighbour one site 'up' are labelled as $\varrho = 2, 4$.

To write down the Hamiltonian in a compact form it is convenient to define the formal index operators of lattice translations, $r(æ)$, $l(æ)$ and $d(æ)$ which, when applied to any lattice site index æ, translate the index to one of the three nearest sites, æ′. These operators, when applied to the lattice site which has one nearest neighbour down, translate the index respectively to the right, left or down from that site. For the lattice sites which have an upper nearest neighbour, one has to turn the lattice upside down before applying these definitions. Notice that the square of each of these three operators is equivalent to the identity operator. So, for example, moving from a lattice site to the right once and then moving to the right again, after flipping the lattice upside down, one returns to the starting site. In particular, for the second

lattice labelling scheme, which we will use below, we have

$$\begin{aligned}
&r(m,n,1)=(m,n,2), && l(m,n,1)=(m,n-1,2), && d(m,n,1)=(m-1,n,4),\\
&r(m,n,2)=(m,n,1), && l(m,n,2)=(m,n+1,1), && d(m,n,2)=(m,n,3),\\
&r(m,n,3)=(m,n+1,4), && l(m,n,3)=(m,n,4), && d(m,n,3)=(m,n,2),\\
&r(m,n,4)=(m,n-1,3), && l(m,n,4)=(m,n,3), && d(m,n,4)=(m+1,n,1).
\end{aligned} \tag{2}$$

Each atom of a carbon nanotube is chemically bound with its three nearest neighbours, and we can define the lattice vectors $\vec{D}_{æ,\delta(æ)}=\vec{R}_{\delta(æ)}-\vec{R}_{æ}$, connecting the atom {æ} with its three nearest neighbours $\delta(æ)$, where $\delta=r,l,d$ are the index translation operators defined above. In what follows, we add the superscript 0 to any quantity when it refers to the equilibrium positions of the atoms. In a 2D graphene sheet the three vectors $\vec{D}^0_{æ,\delta(æ)}$ are coplanar. The valence angles between them are $\phi_0=2\pi/3$ and the equilibrium length of the C–C bond is $|\vec{D}^0_{æ,\delta(æ)}|=d$. In a nanotube these three vectors become noncoplanar and the wrapping can change the valence angles as well as the equilibrium distances between the atoms. It is possible to show that the wrapping of a graphene sheet into a cylinder does not change the equilibrium length d and results in only small deviations of the bond angles from their planar values. The two inequivalent bond angles (the angle between the valence bonds directed along the nanotube axis and wrapped around the tube circumference, ϕ_1, and the one between the bonds which are wrapped around the tube circumference, ϕ_2) become slightly smaller than the planar angle, $\phi_0=2\pi/3$. In consequence, the radius of a tube is slightly larger than that resulting from an ideal rolling of a sheet. These deviations are small $\sim\sin^2\left(\frac{\alpha}{4}\right)$ and can be neglected. So the lattice constant of a 1D periodical nanotube structure, a, and the nanotube radius, R, become

$$\begin{aligned}
&a=2d(1+\sqrt{1-\gamma^2})\approx 3d, \qquad R=\frac{\gamma d}{2\sin\left(\frac{\alpha}{4}\right)}\approx\frac{\sqrt{3}d}{4\sin\left(\frac{\alpha}{4}\right)},\\
&\gamma=\sin(\phi_1)\approx\frac{\sqrt{3}}{2}.
\end{aligned} \tag{3}$$

The azimuthal, $\Theta_{æ}$, and the longitudinal, $z_{æ}$, coordinates of the equilibrium positions of the atoms in a zigzag nanotube are determined by the following expressions:

$$\begin{aligned}
&\Theta_{m,n,1}=n\alpha, && \Theta_{m,n,2}=(n+\tfrac{1}{2})\alpha, && \Theta_{m,n,3}=(n+\tfrac{1}{2})\alpha, && \Theta_{m,n,4}=n\alpha,\\
&z_{m,n,1}=ma-d, && z_{m,n,2}=ma-\tfrac{1}{2}d, && z_{m,n,3}=ma+\tfrac{1}{2}d, && z_{m,n,4}=ma+d.
\end{aligned} \tag{4}$$

The position of the atoms in a nanotube, when they move away from their equilibrium, is given by the radius-vector $\vec{R}_{æ}=\vec{R}^0_{æ}+\vec{U}_{æ}$, where the local displacement vector, $\vec{U}_{æ}$, can be represented through the three orthogonal local vectors [27]:

$$\vec{U}_{æ}=\sum_{\varsigma=1}^{3}u^{\varsigma}_{æ}\vec{e}_{\varsigma}(æ). \tag{5}$$

Here the unit vector $\vec{e}_1(æ)$ is normal to the nanotube surface, $\vec{e}_2(æ)$ is tangential to the cylindrical surface of the nanotube and perpendicular to the nanotube axis, and $\vec{e}_3(æ)$ is tangential to this surface and parallel to the nanotube axis:

$$\vec{e}_1(æ)=\vec{e}_x\sin\Theta_{æ}+\vec{e}_y\cos\Theta_{æ}, \qquad \vec{e}_2(æ)=\vec{e}_x\cos\Theta_{æ}-\vec{e}_y\sin\Theta_{æ}, \qquad \vec{e}_3(æ)=\vec{e}_z. \tag{6}$$

In the case of small displacements, $|\vec{U}_{\delta(æ)}-\vec{U}_{æ}|\ll|\vec{D}^0_{æ,\delta(æ)}|=d$, the distance between the lattice sites is approximately given by $|\vec{D}_{æ,\delta(æ)}|\approx d+W_{æ,\delta(æ)}$, where

$$W_{æ,\delta(æ)}=\vec{r}_{æ,\delta(æ)}\cdot(\vec{U}_{\delta(æ)}-\vec{U}_{æ}), \tag{7}$$

with $\vec{r}_{æ,\delta(æ)}=\vec{D}^0_{æ,\delta(æ)}/|\vec{D}^0_{æ,\delta(æ)}|$ being the unit vector between these two sites. The explicit expressions for $W_{æ,\delta(æ)}$ are given in appendix A.

We can also compute the angle which characterizes the curvature of the deformed lattice, defined as the solid angle spanned by the three lattice vectors located at a given site:

$$S_{æ} = \frac{(\vec{D}_{æ,l(æ)} \times \vec{D}_{æ,r(æ)}) \cdot \vec{D}_{æ,d(æ)}}{|\vec{D}_{æ,l(æ)}||\vec{D}_{æ,r(æ)}||\vec{D}_{æ,d(æ)}|} \approx S^0_{æ} + \frac{1}{d} C_{æ}, \tag{8}$$

where $S^0_{æ} = S^0 = (\vec{r}_{æ,l(æ)} \times \vec{r}_{æ,r(æ)}) \cdot \vec{r}_{æ,d(æ)} = (3/4)\sin(\alpha/2)$ is the equilibrium value, and

$$C_{æ} = \sum_{\delta} \left(\vec{r}_{æ,\delta(æ)} \times \left(\vec{r}_{æ,\delta_1(æ)} \times \vec{r}_{æ,\delta_2(æ)}\right)\right) \cdot (\vec{r}_{æ,\delta(æ)} \times (\vec{U}_{\delta(æ)} - \vec{U}_{æ})) \tag{9}$$

is the deviation from the equilibrium value due to the site displacements. Here $(\delta_1, \delta_2, \delta)$ are cyclic permutations of (l, r, d).

3. Hamiltonian of the system

To study the self-trapped electron states in a nanotube we use the Fröhlich-type Hamiltonian which, in the case of the zigzag tube structure, reads as

$$H = H_{\mathrm{e}} + H_{\mathrm{ph}} + H_{\mathrm{int}} = \sum_{k,\nu,\lambda} E_{\lambda}(k, \nu) c^{\dagger}_{k,\nu,\lambda} c_{k,\nu,\lambda} + \sum_{q,\nu\tau} \hbar\omega_{\tau}(q, \nu) b^{\dagger}_{q,\nu,\tau} b_{q,\nu,\tau}$$
$$+ \frac{1}{\sqrt{12LN}} \sum_{k,q,\nu,\mu,\tau,} \sum_{\lambda,\lambda'} F_{\lambda,\lambda'}(k, \nu; q, \mu|\tau) c^{\dagger}_{k,\nu,\lambda} c_{k-q,\nu-\mu,\lambda'} Q_{q,\mu,\tau}, \tag{10}$$

where k and q are dimensionless wavenumbers (quasi-momenta) along the nanotube which take values $k = \frac{2\pi}{L} n_1$, $L \gg 1$ in the range $(-\pi, \pi]$; $c^{\dagger}_{k,\nu,\lambda}$ $(c_{k,\nu,\lambda})$ and $b^{\dagger}_{q,\nu,\tau}$ $(b_{q,\nu,\tau})$ are creation (annihilation) operators of an electron in the band $E_{\lambda}(k, \nu)$ and of a phonon with the frequency $\omega_{\tau}(q, \nu)$, respectively. Because the unit cell of a tube, as a 1D periodic structure, contains $4N$ atoms there are $4N$ electron bands labelled by two quantum numbers (ν, λ), and $12N$ phonon branches, labelled by (μ, τ). Here ν and μ are azimuthal quantum numbers due to the rotational symmetry which take N discrete values $\nu(\mu) = \frac{2\pi}{N} n_2$ with $n_2 = 0, \pm 1, \ldots, \pm\frac{N-1}{2}$ if N is odd and $n_2 = 0, \pm 1, \ldots, \pm(\frac{N}{2} - 1), \frac{N}{2}$ if N is even. Finally, $\lambda = 1, 2, 3, 4$ and $\tau = 1, 2, \ldots, 12$ due to the existence of four atoms in each cell, as has been mentioned above. The last term in (10) describes the interaction of electrons with phonons where $F_{\lambda,\lambda'}(k, \nu; q, \mu|\tau)$ is the coupling function, and where

$$Q_{q,\nu,\tau} = \sqrt{\frac{\hbar}{2\omega_{\tau}(q, \nu)}} \left(b_{q,\nu,\tau} + b^{\dagger}_{-q,-\nu,\tau}\right). \tag{11}$$

The Hamiltonian (10) is written in the quasi-momentum representation and can be rewritten in the site representation by means of the unitary transformation:

$$a_{æ} \equiv a_{m,n,\varrho} = \frac{1}{2\sqrt{LN}} \sum_{k,\nu,\lambda} \mathrm{e}^{\mathrm{i}km + \mathrm{i}\nu n} v_{\varrho,\lambda}(k, \nu) c_{k,\nu,\lambda},$$
$$\frac{1}{4} \sum_{\varrho} v^{*}_{\varrho,\lambda}(k, \nu) v_{\varrho,\lambda'}(k, \nu) = \delta_{\lambda,\lambda'}, \tag{12}$$

where $a_{æ}$ is the annihilation operator of an electron located on the site $æ \equiv (m, n, \varrho)$. In the site representation the electron Hamiltonian H_{e} in (10) takes the form

$$H_{\mathrm{e}} = \sum_{æ} \left(\mathcal{E}_0 a^{\dagger}_{æ} a_{æ} - \sum_{æ'} J_{æ,æ'} a^{\dagger}_{æ} a_{æ'}\right), \tag{13}$$

where $\mathcal{E}_0$ is the on-site electron energy and $J_{æ,æ'}$ is the energy of the hopping interaction between the sites æ and æ′. Models of carbon nanotubes are normally formulated in a real-space representation which corresponds to the tight-binding approximation. This relatively

simple approximation adequately describes electron states in many physical systems, such as polyacetylene, graphite and carbon nanotubes, as has been successfully demonstrated in numerous papers (see, e.g., [9, 13, 14] and references therein). The electron band structure of an SWCNT has been studied theoretically [28, 18, 29, 30, 12] within the nearest-neighbour hopping approximation. The transformation (12) transforms the electron Hamiltonian H_e^0 into a diagonal form and for a zigzag tube gives 1D electronic bands with the dispersion law [13]

$$E_\lambda(k, \nu) = \mathcal{E}_0 \pm \mathcal{E}_\pm(k, \nu), \tag{14}$$

where

$$\mathcal{E}_\pm(k, \nu) = J_0\sqrt{1 + 4\cos^2\left(\frac{\nu}{2}\right) \pm 4\cos\left(\frac{\nu}{2}\right)\cos\left(\frac{k}{2}\right)}. \tag{15}$$

Below we label the quasiparticle bands as

$$\begin{aligned} E_1(k, \nu) &= \mathcal{E}_0 - \mathcal{E}_+(k, \nu), \qquad & E_2(k, \nu) &= \mathcal{E}_0 - \mathcal{E}_-(k, \nu), \\ E_3(k, \nu) &= \mathcal{E}_0 + \mathcal{E}_-(k, \nu), \qquad & E_4(k, \nu) &= \mathcal{E}_0 + \mathcal{E}_+(k, \nu). \end{aligned} \tag{16}$$

The explicit form of the coefficients $v_{\varrho,\lambda}(k, \nu)$ is given in appendix A.

The electron–phonon interaction originates from different mechanisms [18, 19, 31, 12, 27], one of which, most frequently considered, is related to the dependence of the hopping interaction $J_{æ;\delta(æ)}$ (an off-diagonal term in the Hamiltonian H_e) between the nearest neighbours on their separation. In the linear approximation with respect to the displacements one has

$$J_{æ;\delta(æ)} = J_0 - J_1 W_{æ,\delta(æ)}. \tag{17}$$

Generally, the electron–lattice interaction affects both terms of the electron Hamiltonian (13) [32–35]. Neighbouring atoms alter the electron energy on each site and the lattice displacements create an effective potential, called 'deformational potential', which is proportional to the local contraction/dilatation. In the linear approximation we can write the on-site electron energy as

$$\mathcal{E}_{æ} = \mathcal{E}_0 + \chi_1 \sum_\delta W_{æ,\delta(æ)} + \chi_2 C_{æ}, \tag{18}$$

where χ_1 and χ_2 take into account the dependence of energy on the interatomic distance and on the local nanotube curvature, correspondingly; $W_{æ,\delta(æ)}$ and $C_{æ}$ are given in (7) and (9).

After the transformation (12) and having passed from the lattice displacements to the phonon variables

$$u^\varsigma_{m,n,\varrho} = \frac{1}{\sqrt{12MNL}} \sum_{q,\mu,\tau} e^{i(qm+\mu n)} U_{\varsigma,\varrho;\tau}(q, \mu) Q_{q,\mu,\tau}, \tag{19}$$

we obtain the interaction Hamiltonian $H_{\rm int}$ in (10) with the electron–phonon coupling function $F_{\lambda,\lambda'}(k, \nu; q, \mu|\tau)$, which is determined by the interaction parameters χ_1, χ_2, J_1 and by the coefficients of the unitary transformations (12) and (19). The expression for $F_{\lambda,\lambda'}(k, \nu; q, \mu|\tau)$ is given in appendix A.

The explicit expressions for coefficients of the transformation (19), as well as for the phonon frequencies $\omega_\tau(q, \mu)$ can be found from the diagonalization requirement of the potential energy of the lattice displacements (for a review of phonon modes in carbon nanotubes see, e.g., [13]). In the harmonic approximation the potential energy is

$$V_{\rm lat} = \tfrac{1}{2} \sum_{æ,æ'} (\vec{U}_{æ'} - \vec{U}_{æ}) K^{(æ,æ')} (\vec{U}_{æ'} - \vec{U}_{æ}), \tag{20}$$

where $K^{(æ,æ')}$ is an interatomic-force-constant tensor. Any deformation can be represented as a sum of a compressive deformation at which the distances between atoms are changed, and of a

shear strain for which the interatomic distances are unchanged. In the case of a 2D lattice, e.g., of a graphene sheet, these deformations correspond to the in-plane displacements. Clearly, the out-of-plane displacements lead to the deviation of the solid angle spanned by the three lattice vectors located at a given site from the equilibrium value, (9). Therefore, we also introduce a constant w_c which describes such a deformation. The corresponding three constants, the compressive modulus w, the modulus of elasticity in a shear $w_\perp$, and w_c, guarantee the lattice stability even in the nearest-neighbour interaction approximation. In this case the summation in (20) is taken over the nearest neighbours, i.e., $æ' = \delta(æ)$, and the tensor $K^{(æ,æ')}$ is given by

$$K^{(æ,æ')} = \frac{w}{2}\vec{r}_{æ,\delta(æ)}\vec{r}_{æ,\delta(æ)} + \frac{w_\perp}{2}\vec{r}^{\perp}_{æ,\delta(æ)}\vec{r}^{\perp}_{æ,\delta(æ)} + w_c K_c^{(æ,æ')}. \tag{21}$$

Here $K_c^{(æ,æ')}$ is a tensor corresponding to the deformations (9), $\vec{r}\vec{r}$ is a dyad, and the vector $\vec{r}^{\perp}_{æ,\delta(æ)}$ is a unit vector orthogonal to $\vec{r}_{æ,\delta(æ)}$ and defined as

$$\vec{r}^{\perp}_{æ,\delta(æ)} = \vec{r}_{æ,\delta(æ)} \times \vec{n}_{æ,\delta(æ)}, \qquad \vec{n}_{æ,\delta(æ)} = \vec{e}_x \sin\left(\frac{\Theta_{\delta(æ)} + \Theta_{æ}}{2}\right) + \vec{e}_y \cos\left(\frac{\Theta_{\delta(æ)} + \Theta_{æ}}{2}\right), \tag{22}$$

where $\vec{n}_{æ,\delta(æ)}$ is a unit vector normal to the nanotube surface and orthogonal to $\vec{r}_{æ,\delta(æ)}$.

Usually we have $w \geqslant w_\perp \gg w_c$; for instance, in carbon nanotubes $w_\perp/w \approx 0.7$ [13]. To reduce the number of the system parameters, we put $w_\perp = w$. Then, the phonon Hamiltonian in our model becomes

$$H_{ph} = \frac{1}{2}\sum_{æ}\left(\frac{\vec{P}^2_{æ}}{M} + \frac{1}{2}w\sum_{\delta}\left(W^2_{æ,\delta(æ)} + \Omega^2_{æ,\delta(æ)}\right) + w_c C^2_{æ}\right), \tag{23}$$

where $\vec{P}_{æ}$ is the momentum, canonically conjugate to the displacement $\vec{U}_{æ}$, $W_{æ,\delta(æ)}$ and $C_{æ}$ are defined in (7) and (9), and $\Omega_{æ,\delta(æ)}$ is defined as

$$\Omega_{æ,\delta(æ)} = \vec{r}^{\perp}_{æ,r(æ)} \cdot (\vec{U}_{\delta(æ)} - \vec{U}_{æ}) \tag{24}$$

whose explicit form is given in appendix A.

After applying the transformation (19), the diagonalization requirement of the potential energy of the lattice displacements in (23) becomes

$$\frac{1}{12M}\sum_{\varrho}\left[\frac{w}{2}\sum_{\delta}\left(W^*_{\varrho,\delta(\varrho)}(q,\mu,\tau)W_{\varrho,\delta(\varrho)}(q,\mu,\tau') + \Omega^*_{\varrho,\delta(\varrho)}(q,\mu,\tau)\Omega_{\varrho,\delta(\varrho)}(q,\mu,\tau')\right) + w_c C^*_{\varrho}(q,\mu,\tau)C_{\varrho}(q,\mu,\tau')\right] = \omega^2_{\tau}(q,\mu)\,\delta_{\tau,\tau'}. \tag{25}$$

Here $W_{æ,\delta(æ)}$, $\Omega_{æ,\delta(æ)}$, and $C_{æ}$ are the linear forms of the transformation coefficients $U_{\varsigma,\varrho;\tau}(q,\mu)$ for $W_{æ,\delta(æ)}$, $\Omega_{æ,\delta(æ)}$, and $C_{æ}$, respectively.

The equations for the normal modes of lattice vibrations are too complicated, in the general case, to be solved analytically. For carbon nanotubes the phonon modes were calculated numerically (see, e.g., [13, 27] and references therein). Here we aim to study the self-trapped states of an extra electron in such systems. To get the equation for the electron wavefunction in the adiabatic approximation, we do not calculate the phonon spectrum explicitly; instead, we use the general relation (25) and the orthonormalization conditions for the coefficients of the unitary transformation (19).

A neutral carbon nanotube contains $4NL$ electrons, i.e., it is a half-filled band system with one electron per atom. The energy dispersion relations (14)–(15), based on the tight-binding approximation Hamiltonian (13), describe the one-electron band structure of a zigzag nanotube where the electron–electron interaction is ignored. Such a relatively simple model has

successfully predicted conducting properties (metallic or semiconducting) of carbon nanotubes depending on N [13, 14, 24, 18, 25]. Moreover, the Hamiltonian (10) also effectively describes an extra electron in such a system if the electron–electron correlation is taken into account. Indeed, some experimental facts indicate that in carbon nanotubes such correlations are significant. Some theoretical studies within the Hubbard model [36–38] provide some concrete predictions that are supported experimentally. In particular, (i) in carbon nanotubes the electron–electron interaction causes superconducting fluctuations [39] as predicted in [37]; (ii) the temperature dependence of the resistance of SWCNTs [40] in a broad interval of temperature is consistent with the theoretical predictions at 'a rather large bare Hubbard interaction, $u/t \sim 10$' (in our notation V_0/J_0) [38]; (iii) in carbon nanotubes the energy level of an extra electron (affinity electron) is much higher than that of the nanotube intrinsic electrons, as follows from the comparison of the ionization energy of carbon atoms, which is 11.26 eV, and the electron affinity energy, which is 1.27 eV, so the on-site Coulomb repulsion energy can be estimated as 10 eV, which is significantly bigger than J_0. Therefore, such a system can be effectively described by the Hamiltonian (13). Finally, an extra argument to justify the validity of our model in describing one extra electron in carbon nanotubes is provided by the exact solution of the 1D Hubbard model given in appendix B.

4. Self-trapped quasiparticle states

The self-trapped states of a quasiparticle are usually described in the adiabatic approximation in which the state of the system is represented in the multiplicative Born–Oppenheimer form,

$$|\Psi\rangle = U\,|\psi_{\mathrm{e}}\rangle, \tag{26}$$

where U is the unitary operator of the coherent atom displacements induced by the presence of the quasiparticle:

$$U = \exp\left[\sum_{\mu,q,\tau}(\beta_\tau(q,\mu)b^\dagger_{q,\mu,\tau} - \beta^*_\tau(q,\mu)b_{q,\mu,\tau})\right], \tag{27}$$

and $|\psi_{\mathrm{e}}\rangle$ is the state-vector of the quasiparticle,

$$|\psi^{(0)}_{\mathrm{e}}\rangle = \sum_{\lambda,\nu,k}\psi_\lambda(k,\nu)c^\dagger_{k,\nu,\lambda}|0\rangle = \sum_{æ}\psi_{æ}a^\dagger_{æ}|0\rangle. \tag{28}$$

Here $|0\rangle$ is the vacuum state of the quasiparticle and of the phonons; $\psi_\lambda(k,\nu)$ and $\psi_{æ}$ are the quasiparticle wavefunctions in the momentum and the site representations, respectively. They are connected by the unitary transformation:

$$\psi_{æ} \equiv \psi_{m,n,\varrho} = \frac{1}{2\sqrt{LN}}\sum_{\lambda,\nu,k}\mathrm{e}^{\mathrm{i}(km+\nu n)}v_{\varrho,\lambda}(k,\nu)\psi_\lambda(k,\nu) \tag{29}$$

and satisfy the normalization conditions

$$\langle\psi_{\mathrm{e}}|\psi_{\mathrm{e}}\rangle = \sum_{\lambda,\nu,k}|\psi_\lambda(k,\nu)|^2 = \sum_{æ}|\psi_{æ}|^2 = 1. \tag{30}$$

In the adiabatic approximation the lattice kinetic energy is considered as a perturbation and the adiabatic lattice displacements are taken into account by the unitary transformation (27). The resulting Hamiltonian consists of the two terms, $H = H_0 + H_{na}$, of which one describes the adiabatic electron states in the self-consistent lattice potential and the other represents the residual, nonadiabatic, electron–phonon interaction (see, e.g., [41] and references therein). Generally speaking, the adiabatic approximation works well at a relatively strong electron–phonon coupling [41, 23]. To prove its validity explicitly for a particular system, one has to

calculate the higher-order corrections to the total energy of the system and compare them with the zero-order adiabatic approximation, which will be done in our next study.

The adiabatic approximation is equivalent to the semiclassical consideration in which the vibrational subsystem is treated as a classical one. Considering $\langle\Psi|H|\Psi\rangle$ as the Hamiltonian functional of the quasiparticle wavefunction and of the lattice variables we obtain a system of equations which describes the interconnections between the quasiparticle and the phonon subsystems. The numerical studies of such systems are normally carried out in the site representation. Here we prefer to use the momentum representation in which the resultant system of equations reads as

$$E\psi_\lambda(k,\nu) = E_\lambda(k,\nu)\psi_\lambda(k,\nu) + \frac{1}{\sqrt{12LN}}\sum_{q,\lambda',\tau,\mu} F_{\lambda,\lambda'}(k,\nu;q,\mu|\tau)\bar{Q}_\tau(q,\mu)\psi_{\lambda'}(k-q,\nu-\mu), \tag{31}$$

$$\omega_\tau^2(q,\mu)\bar{Q}_\tau(q,\mu) = -\frac{1}{\sqrt{12LN}}\sum_{k,\nu,\lambda,\lambda'} F^*_{\lambda,\lambda'}(k,q;\nu,\mu|\tau)\psi^*_{\lambda'}(k-q,\nu-\mu)\psi_\lambda(k,\nu), \tag{32}$$

where

$$\bar{Q}_\tau(q,\mu) = \langle\Psi|Q_\tau(q,\mu)|\Psi\rangle = \sqrt{\frac{\hbar}{2\omega_\tau(q,\mu)}}\left(\beta_\tau(q,\mu) + \beta^*_\tau(-q,-\mu)\right). \tag{33}$$

Substituting (32) into equations (31), we obtain a system of nonlinear equations for the wavefunctions $\psi_\lambda(k,\nu)$

$$(E_\lambda(k,\nu) - E)\psi_\lambda(k,\nu) = \frac{1}{LN}\sum_{\lambda',\lambda'_1,\lambda_1,k_1,\nu_1,q,\mu} G^{\lambda'_1,\lambda_1}_{\lambda,\lambda'}\begin{pmatrix} k, & k_1, & q \\ \nu, & \nu_1, & \mu \end{pmatrix} \times \psi^*_{\lambda'_1}(k_1-q,\nu_1-\mu)\psi_{\lambda_1}(k_1,\nu_1)\psi_{\lambda'}(k-q,\nu-\mu). \tag{34}$$

Their solution gives the wavefunctions $\psi_\lambda(k,\nu)$ and the eigenenergy E of the quasiparticle ground state and, therefore, the self-consistent lattice distortion (32). Here we have introduced the notation

$$G^{\lambda'_1,\lambda_1}_{\lambda,\lambda'}\begin{pmatrix} k, & k_1, & q \\ \nu, & \nu_1, & \mu \end{pmatrix} = \frac{1}{12}\sum_\tau \frac{F_{\lambda,\lambda'}(k,\nu;q,\mu|\tau)F^*_{\lambda_1,\lambda'_1}(k_1,\nu_1;q,\mu|\tau)}{\omega^2_\tau(q,\mu)}. \tag{35}$$

We would like to point out here that while in the case of a simple chain with a single energy band one-quasiparticle self-trapped states are described by a nonlinear equation, in a complex quasi-1D system with several quasiparticle energy bands, we have a system of nonlinear equations. All sublevels of all (sub)bands participate in the formation of these self-trapped electron states and, as a result, there are many solutions of equation (34). System (34) also admits 'one-band' solutions $\psi_\lambda(k,\nu) = \psi(k)\delta_{\lambda,\lambda_0}\delta_{\nu,\nu_0}$. Therefore, in the case of such a 'one-band' solution, the probability amplitude in the site representation

$$\psi_{m,n,\varrho} = \frac{1}{2\sqrt{LN}}\sum_k \mathrm{e}^{\mathrm{i}km}\mathrm{e}^{\mathrm{i}\nu_0 n}v_{\varrho,\lambda_0}(k,\nu_0)\psi(k) = \psi_{m,n,\varrho;\lambda_0,\nu_0} \tag{36}$$

depends on the particular band in which the soliton state is formed. Having the same k-dependence of the solution $\psi(k)$, the electron distribution can be different for different bands. Note also that for a 'one-band' solution, according to (32), only the azimuthal symmetrical distortion of the nanotube takes place, i.e., $\bar{Q}_\tau(q,\mu) = \bar{Q}_\tau(q)\delta_{\mu,0}$. Therefore, a 'one-band' solution describes azimuthally symmetric self-trapped states with a spontaneously broken translational symmetry. Not all of these 'one-band' solutions are stable. For example, nanotube electronic subbands (16) with $\nu \neq 0$ are doubly degenerate and, as a result, the energy levels

of the two 'one-band' self-trapped states with different azimuthal numbers ($\nu = \nu_0$ and $-\nu_0$) are degenerate. Consequently, according to the Jahn–Teller theorem, these states are unstable with respect to the lattice distortions which reduce the symmetry and remove the degeneracy of these states. As shown in [42], the Jahn–Teller effect plays a significant role in the optical properties of nanosystems.

The most stable state is the state which is split from the lowest energy subband in (16), namely from $E_1(k, 0)$ with $\lambda = 1$ and $\nu = 0$. This band is nondegenerate, and its bottom is sufficiently far from the energy of other bands. We assume that in the site representation a solution is given by a broad enough wave packet and is formed by the states with small values of quasi-momentum. Therefore, the states from higher energy bands can be ignored and we can use the 'one-band' approximation and seek a solution in the form $\psi_\lambda(k, \nu) = \psi(k)\delta_{\lambda,1}\delta_{\nu,0}$. These assumptions allow us to use the long-wave approximation:

$$\begin{aligned} E_1(k, 0) &= \mathcal{E}_0 - J_0\sqrt{5 + 4\cos\left(\frac{k}{2}\right)} \approx E_1(0) + \frac{1}{12}J_0k^2, \\ G^{1,1}_{1,1}\begin{pmatrix} k, & k_1, & q \\ 0, & 0, & 0 \end{pmatrix} &\approx G^{1,1}_{1,1}\begin{pmatrix} 0, & 0, & 0 \\ 0, & 0, & 0 \end{pmatrix} \equiv G_0. \end{aligned} \tag{37}$$

Here

$$E_1(0) = \mathcal{E}_0 - 3J_0 \tag{38}$$

is the energy bottom of the subband $E_1(k, 0)$,

$$G_0 = a_1^2\frac{3[(\chi_1 + J_1)^2 + b_1^2\chi_2^2 + b_2(\chi_1 + J_1)\chi_2]}{4w} = p^2\frac{3(\chi_1 + J_1)^2}{4w}, \tag{39}$$

where $p^2 = a_1^2[(\chi_1 + J_1)^2 + b_1^2\chi_2^2 + b_2(\chi_1 + J_1)\chi_2]/(\chi_1 + J_1)^2$, $a_1^2 = w/(w + c_1^2w_c)$, and b_1^2, $|b_2|$, c_1^2 are constants $\leqslant 1$. To obtain (39), we have used the explicit expressions (35), the orthonormalization conditions for the coefficients of the unitary transformations and have assumed that $w > w_c$.

To solve the nonlinear equation for $\psi(k)$ we introduce the function

$$\varphi_0(\zeta) = \frac{1}{\sqrt{L}}\sum_k e^{ikx}\psi(k), \tag{40}$$

which depends on the continuous variable ζ, which is a dimensionless coordinate along the nanotube axis related to z by the relation $\zeta = z/3d$. Because of (30), $\varphi_0(\zeta)$ satisfies the normalization condition

$$\int_{-L/2}^{L/2} |\varphi_0(\zeta)|^2\, d\zeta = 1. \tag{41}$$

Then, using the long-wave approximation (37), we can transform the equation for $\psi(k)$ into a differential equation for $\varphi(\zeta)$:

$$\frac{d^2\varphi_0(\zeta)}{d\zeta^2} + \lambda_0\varphi_0(\zeta) + 4g_0|\varphi_0(\zeta)|^2\varphi_0(\zeta) = 0, \tag{42}$$

which is the well-known stationary nonlinear Schrödinger equation (NLSE). Here

$$\lambda_0 = \frac{12(E - \mathcal{E}_0 + 3J_0)}{J_0}, \qquad g_0 = \frac{9p^2(\chi_1 + J_1)^2}{4NJ_0w} = \frac{9\sigma}{4N}, \tag{43}$$

where we have introduced the dimensionless electron–phonon coupling constant:

$$\sigma = \frac{p^2(\chi_1 + J_1)^2}{J_0w}. \tag{44}$$

A normalized solution of the NLSE is given by the function

$$\varphi_0(\zeta) = \sqrt{\frac{g_0}{2}}\frac{1}{\cosh(g_0(\zeta-\zeta_0))} \tag{45}$$

with $\lambda_0 = -g_0^2$. The eigenenergy of this state is

$$E_0 = E_1(0) - \frac{J_0 g_0^2}{12} = E_1(0) - \left(\frac{3}{4}\right)^3 \frac{\sigma^2 J_0}{N^2}. \tag{46}$$

The probability amplitude (36) of a self-trapped quasiparticle distribution over the nanotube sites is given by the function

$$\psi_{m,n,\varrho} = \frac{1}{2\sqrt{LN}}\sum_k \mathrm{e}^{\mathrm{i}km} v_{\varrho,1}(k,0)\psi(k). \tag{47}$$

The explicit expressions for $v_{\varrho,1}(k,0)$ are given below in (86). In the long-wave approximation for the phase $\theta_+(k,0)$ we find from (87) that $\theta_+(k,0) \approx k/12$. Then, using the expressions for $v_{\varrho,1}(k,0)$ and taking into account the definition (40), we obtain

$$\psi_{m,n,\varrho} = \frac{1}{2\sqrt{N}}\varphi_0(z_{m,\varrho}), \tag{48}$$

where $z_{m,\varrho}$ describes the atom positions along the nanotube axis (4).

According to our solution (45) the quasiparticle probability distribution over the nanotube sites is given by the expression

$$P_{\varrho,m,n} = \frac{1}{4N}|\varphi_0(z_{m,\varrho})|^2 = \frac{g_0}{8N}\frac{1}{\cosh^2\left(g_0 z_{m,\varrho}/3d\right)}. \tag{49}$$

Thus, the quasiparticle is localized along the tube axis in the domain $\Delta z = 3\pi d/g_0 = 4\pi d N/(3\sigma)$, and is uniformly distributed over the azimuthal angle of the tube. The sum

$$\sum_n P_{\varrho,m,n} = P_{\varrho,m} = \frac{1}{4}|\varphi_0(z_{m,\varrho})|^2 = \frac{g_0}{8}\frac{1}{\cosh^2\left(g_0 z_{m,\varrho}/3d\right)} \tag{50}$$

gives the quasiparticle distribution along the tube axis and describes a large quasi-1D polaron. In this state, as well as in other 'one-band' states, according to (32), only the total symmetrical distortion of the nanotube takes place, i.e., $Q_\tau(q,0) \neq 0$ with $\mu = 0$ and $Q_\tau(q,\mu) = 0$ for $\mu \neq 0$. The distortion itself can be calculated explicitly by substituting the obtained quasiparticle functions into equation (32). The corresponding solution shows that the main characteristics of this distortion are the radial displacements of atoms as the longitudinal ones are smaller and the tangential displacements vanish. Using equations (5), (32) and (33) we obtain the following expression for the radial components of the distortion:

$$\bar{u_r} = \langle\Psi|u^1_{\mathrm{ae}}|\Psi\rangle \approx -\frac{\sqrt{3}p(\chi_1+J_1)g_0}{16Nw\sin\frac{\alpha}{4}\cosh^2\left(g_0 z_{m,\varrho}/3d\right)}. \tag{51}$$

The total energy of such a polaron state including the energy of the lattice deformation, W, is

$$\mathcal{E}_{\mathrm{tot}} = \langle\Psi|H|\Psi\rangle = W + E_0 = E_1(0) - \left(\frac{3}{4}\right)^3 \frac{\sigma^2 J_0}{3N^2}. \tag{52}$$

As we see, our solution in the long-wave approximation is azimuthally symmetric and describes a large quasi-1D polaron state. The energy of the polaron state, as well as the extent of the quasiparticle localization along the nanotube axis, depends on the electron–phonon coupling and on the diameter of the nanotube. It follows from equation (46) that the energy gap between the adiabatic ground and excited states decreases as the nanotube diameter

increases. At large N this gap is small, nonadiabatic corrections become essential, and strong hybridization of the ground and the excited states takes place [41]. In this case the adiabatic approach becomes invalid and the 1D polaron is unstable.

When the electron–phonon coupling increases, the region of localization gets smaller. Consequently, the wave packet in the quasi-momentum representation becomes broader and the electron states with higher energies can participate in the formation of the polaron state. At strong enough coupling the electron states from the upper bands, $\nu \neq 0$, can also contribute to the polaron formation, which then can lead to the breakdown of the azimuthal symmetry of the solution.

5. Transition to states with broken axial symmetry

To consider the transition from a 1D large polaron state to the one with a broken azimuthal symmetry, it is necessary to take into account the higher energy bands. For this we perform the partial transformation of equations (34) into the site representation. In the zigzag nanotubes, one can identify zigzag chains of $2N$ carbon atoms, with two atoms per unit cell, which encircle the nanotube. We can enumerate atoms as (j, n, ρ), where j enumerates zigzag chains, and $\rho = A, B$ enumerates atoms in the chain unit cell. Let us enumerate the zigzag ring chains in such a way that the even chains, $j = 2m$, consist of atoms $(m, n, 1)$ and $(m, n, 2)$ and the odd chains $j + 1 = 2m + 1$ involve atoms $(m, n, 3)$ and $(m, n, 4)$. Then the chains (rings) with odd number $j - 1 = 2(m - 1) + 1$ include the atoms $(m - 1, n, 3)$ and $(m - 1, n, 4)$. The atoms of the jth chain are equivalent except that the atoms with $\rho = A$ are coupled to the B-atoms of the $(j - 1)$th chain, and those with $\rho = B$ to the A-atom of the $(j + 1)$th chain, and these two sets of atoms are shifted with respect to each other in the opposite directions from the central line, z_j, which is the symmetry line of the chain.

Introducing the functions

$$\phi_{m,\varrho}(\nu) = \frac{1}{2\sqrt{L}} \sum_{\lambda,k} \mathrm{e}^{\mathrm{i}km} v_{\varrho,\lambda}(k, \nu)\psi_\lambda(k, \nu) \tag{53}$$

and the notation

$$\begin{aligned} &\phi_{m,1}(\nu) = \phi_{j,A}(\nu), \qquad \mathrm{e}^{-\mathrm{i}\frac{\nu}{2}}\phi_{m,2}(\nu) = \phi_{j,B}(\nu), \qquad \phi_{m,4}(\nu) = \phi_{j+1,B}(\nu), \\ &\mathrm{e}^{-\mathrm{i}\frac{\nu}{2}}\phi_{m,3}(\nu) = \phi_{j+1,A}(\nu), \qquad \phi_{m-1,4}(\nu) = \phi_{j-1,B}(\nu), \qquad \mathrm{e}^{-\mathrm{i}\frac{\nu}{2}}\phi_{m-1,3}(\nu) = \phi_{j-1,A}(\nu), \end{aligned} \tag{54}$$

we can transform equations (34) as follows:

$$\begin{aligned} E\phi_{j,A}(\nu) = {} & \mathcal{E}_0\phi_{j,A}(\nu) - 2J_0 \cos\left(\frac{\nu}{2}\right)\phi_{j,B}(\nu) - J_0\phi_{j-1,B}(\nu) \\ & - \frac{3p^2\chi_1}{2wN} \sum_{\nu_1,\mu} \Bigg[\chi_1 \left(\phi^*_{j,A}(\nu_1 - \mu)\phi_{j,A}(\nu_1) + \cos\frac{\mu}{2}\phi^*_{j,B}(\nu_1 - \mu)\phi_{j,B}(\nu_1) \right) \\ & + J_1 \Bigg(\cos\frac{\nu_1 - \mu}{2}\phi^*_{j,B}(\nu_1 - \mu)\phi_{j,A}(\nu_1) \\ & + \cos\frac{\nu_1}{2}\phi^*_{j,A}(\nu_1 - \mu)\phi_{j,B}(\nu_1) \Bigg) \Bigg] \phi_{j,A}(\nu - \mu) \\ & - \frac{3p^2 J_1}{2wN} \sum_{\nu_1,\mu} \Bigg[\chi_1 \Bigg(\cos\frac{\nu - \mu}{2}\phi^*_{j,A}(\nu_1 - \mu)\phi_{j,A}(\nu_1) \\ & + \cos\frac{\nu}{2}\phi^*_{j,B}(\nu_1 - \mu)\phi_{j,B}(\nu_1) \Bigg) \end{aligned}$$

$$+ J_1\Bigg(\cos\frac{\nu-\nu_1}{2}\phi^*_{j,B}(\nu_1-\mu)\phi_{j,A}(\nu_1) + \cos\frac{\nu+\nu_1-\mu}{2}\phi^*_{j,A}(\nu_1-\mu)\phi_{j,B}(\nu_1)\Bigg)\Bigg]\phi_{j,B}(\nu-\mu). \tag{55}$$

Similar equations are obtained for $\phi_{j,B}(\nu)$ with the replacement $\phi_{j,A} \to \phi_{j,B}$, $\phi_{j,B} \to \phi_{j,A}$ and $\phi_{j-1,B} \to \phi_{j+1,A}$.

In the derivation of these equations we have used the explicit expressions (35) and the orthonormalization conditions for the coefficients of the unitary transformations of the quasiparticle and phonon subsystems and we have made the qualitative estimate that $w_c \ll w$ and $\chi_2^2 \ll (\chi_1 + J_1)^2$, and, therefore, that $p \sim 1$ in equation (55).

To find the lowest energy state, we look for a solution of equation (55) in the form

$$\phi_{j,\rho}(\nu) = A_{j,\rho}\phi(\nu), \tag{56}$$

where $\phi(\nu)$ satisfies the normalization condition

$$\sum_\nu |\phi(\nu)|^2 = 1, \tag{57}$$

and $A_{j,\rho}$ is the probability amplitude of the quasiparticle distribution on the ρth atom in the jth zigzag chain:

$$\sum_\nu |\phi_{j,\rho}(\nu)|^2 = \sum_\nu |\phi_{m,\varrho}(\nu)|^2 = |A_{j,\rho}|^2 \equiv |A_{m,\varrho}|^2. \tag{58}$$

For an azimuthally symmetric solution the only nonzero functions are those with zero argument: $\phi(\nu) = \delta_{\nu,0}$. Assuming that $A_{j,\rho} = A(\zeta_{j,\rho})$ is a smooth function of a dimensionless variable ζ in the units of the lattice constant $3d$, we can use the continuum approximation, taking into account that $\zeta_{j,B} = \zeta_{j,A} + \frac{1}{6}$, $\zeta_{j-1,B} = \zeta_{j,A} - \frac{1}{3}$. This transforms equation (55) into the continuum NLSE (42) for the function $\varphi(\zeta)$, which has been considered above, where, according to (48), $A(\zeta_{j,\rho}) = (1/2)\varphi(z_{m,\varrho})$. Therefore, for the amplitudes $A_{\rho,j}$ we can use the solution (45). Let the centre of the localization of the azimuthally symmetric solution, ζ_0, in equation (45) correspond to the central line of the j_0th zigzag chain (for simplicity we label it as $j_0 = 0$). According to (45), we then find that

$$\begin{aligned} A_{0,A} &= A_{0,B} = A_0 = \sqrt{\frac{g_0}{8}}\frac{1}{\cosh(g_0/12)}, \\ A_{1,B}(0) &= A_{-1,B}(0) = A_1 = \sqrt{\frac{g_0}{8}}\frac{1}{\cosh(5g_0/12)}. \end{aligned} \tag{59}$$

$$A_{1,A}(0) = A_{-1,A}(0) = A_2 = \sqrt{\frac{g_0}{8}}\frac{1}{\cosh(7g_0/12)}. \tag{60}$$

Thus, the inequalities $A_2/A_0 < A_1/A_0 < 1$ hold.

Next, we consider equation (55) for a chain in which the quasiparticle is mainly localized, i.e., $j = 0$, and we use the ansatz (56). We assume that the solution is close to being azimuthally symmetric, i.e., that the function $\phi(\nu)$ is nonzero only in the vicinity of the zero values of ν. Then, we can use the long-wave approximation $\cos(\nu/2) \approx 1 - (1/2)(\nu/2)^2$ in equation (55). To solve this equation, we introduce a function of the continuum variable x:

$$\varphi(x) = \frac{1}{\sqrt{2N}}\sum_\nu e^{i\frac{\nu}{2}x}\phi(\nu), \tag{61}$$

which is periodic with the period $2N$, $\varphi(x + 2N) = \varphi(x)$, and which, due to (57), satisfies the normalization condition

$$\int_0^{2N} |\varphi(x)|^2\,dx = 1. \tag{62}$$

Note also that the discrete values of $x = l$, $l = 0, 1, 2, \ldots 2N - 1$, in (61) correspond to the atom positions in the zigzag ring (the even numbers, $l = 2n$, correspond to the A-atoms and the odd ones, $l = 2n + 1$, to the B-atoms in the chain $j = 0$).

Using the ansatz (56) and the long-wave approximation, one can transform equation (55) into a nonlinear differential equation for $\varphi(x)$ (stationary NLSE):

$$\frac{\mathrm{d}^2\varphi(x)}{\mathrm{d}x^2} + \lambda_1\varphi(x) + 2g_1|\varphi(x)|^2\varphi(x) = 0, \tag{63}$$

where

$$\lambda_1 = \frac{E - \mathcal{E}_0 + (2+\eta)J_0}{J_0}, \qquad g_1 = \frac{3A_0^2p^2(\chi_1 + J_1)^2}{J_0 w} = 3A_0^2\sigma, \qquad \eta = \frac{A_1}{A_0}. \tag{64}$$

Here σ is the dimensionless electron–phonon coupling constant defined in (44).

Equation (63), which was considered in [43], describes a self-consistent state in a nanocircle. As it was shown there, a periodic solution of equation (63), satisfying the normalization condition (62), is given in terms of the elliptic Jacobi functions:

$$\varphi(x) = \frac{\sqrt{g_1}}{2\mathbf{E}(k)}\mathrm{d}n\left[\frac{2\mathbf{K}(k)x}{2N}, k\right]. \tag{65}$$

Here $\mathbf{K}(k)$ and $\mathbf{E}(k)$ are, respectively, the complete elliptic integrals of the first and second kind [44]. The modulus of the elliptic Jacobi function, k, is determined from the relation

$$\mathbf{E}(k)\mathbf{K}(k) = \frac{g_1 N}{2}. \tag{66}$$

The eigenvalue of the solution (65) is

$$\lambda_1 = -\frac{g_1^2}{4}\frac{(2-k^2)}{E^2(k)}. \tag{67}$$

According to [43], relation (66) holds, and so equation (63) admits such solutions only when g_1 exceeds the critical value of the nonlinearity constant: $g_1 > g_{\mathrm{cr}} = \pi^2/(2N)$. Therefore, at these values of g_1 the azimuthally symmetrical solution is unstable. This determines the critical value of the electron–phonon coupling constant σ above which the solutions with the broken azimuthal symmetry first appear. Taking into account (64), (59) and (43), we obtain the condition for the existence of states with a broken azimuthal symmetry for the nanotubes of an arbitrary radius:

$$\frac{\sigma}{\cosh(3\sigma/16N)} > \frac{4\pi}{3\sqrt{3}}. \tag{68}$$

From here we find that for nanotubes of large enough radius, $N \geqslant 6$, so that $3\sigma/16N \ll 1$, the critical value of the electron–phonon coupling constant (44) does not depend on the nanotube diameter:

$$\sigma_{\mathrm{cr},1} = \frac{4\pi}{3\sqrt{3}} \approx 2.42. \tag{69}$$

Above the values for this transition, the formation of a 2D small polaron on the nanotube surface is possible. Indeed, we can transform equation (55) to the site representation taking into account (54):

$$\begin{aligned} E\psi_{m,n,1} = {} & \mathcal{E}_0\psi_{m,n,1} - J_0(\psi_{m,n,2} + \psi_{m,n-1,2} + \psi_{m-1,n,4}) \\ & - \frac{3a^2}{4w}\Big[\chi_1^2\left(|\psi_{m,n,1}|^2 + |\psi_{m,n,2}|^2 + |\psi_{m,n-1,2}|^2\right)\psi_{m,n,1} \\ & + \chi_1 J_1\big(\left(\psi^*_{m,n,2} + \psi^*_{m,n-1,2}\right)\psi^2_{m,n,1} + 2|\psi_{m,n,1}|^2\left(\psi_{m,n,2} + \psi_{m,n-1,2}\right) \\ & + \psi^*_{m,n,1}\left(\psi^2_{m,n,2} + \psi^2_{m,n-1,2}\right)\big) \\ & + J_1^2\left(\left(|\psi_{m,n,2}|^2 + |\psi_{m,n-1,2}|^2\right)\psi_{m,n,1} + \psi^*_{m,n,1}\left(\psi^2_{m,n,2} + \psi^2_{m,n-1,2}\right)\right)\Big]. \end{aligned} \tag{70}$$

We can consider $\psi_{m,n,\varrho} = \psi(y_{m,n,\varrho}, z_{m,n,\varrho})$ as a function of the coordinates of the atom positions along the nanotube axis, $z_{m,n,\varrho}$, and in the perpendicular direction on the nanotube surface, $y_{m,n,\varrho}$. Defining y and z as the dimensionless coordinates in units of d, we get $\psi(y_{m,n,1}, z_{m,n,1}) = \psi(y, z)$, $\psi(y_{m,n,2}, z_{m,n,2}) = \psi(y + \sqrt{3}/2, z + 1/2)$, $\psi(y_{m,n-1,2}, z_{m,n-1,2}) = \psi(y - \sqrt{3}/2, z + 1/2)$, $\psi(y_{m-1,n,4}, z_{m-1,n,4}) = \psi(y, z - 1)$. In the class of smooth functions we can use the continuum approximation which transforms equation (70) into the stationary 2D modified NLSE (2D MNLSE) for the function $\psi_{m,n,\varrho} = \psi(y, z)$ that satisfies the normalization condition $\sum_{m,n,\varrho} |\psi_{m,n,\varrho}|^2 = 1$. Taking into account that a step along the nanotube axis (summation over m) is $3d$ and a step in the perpendicular direction (summation over n) is $\sqrt{3}d$, we perform the transition from the summation to the integration:

$$\sum_{m,n,\varrho} |\psi_{m,n,\varrho}|^2 \to \sum_{\varrho} \frac{1}{3\sqrt{3}} \int\int |\psi_{\varrho}(y, z)|^2 \, \mathrm{d}z \, \mathrm{d}y$$

$$= \frac{4}{3\sqrt{3}} \int_{-3L/2}^{3L/2} \mathrm{d}z \int_0^{\sqrt{3}N} \mathrm{d}y |\psi(y, z)|^2 = 1. \tag{71}$$

From (70) we can obtain the following 2D MNLSE:

$$\lambda\varphi + \Delta\varphi + 2g_2 \left(|\varphi|^2 + \gamma \Delta |\varphi|^2\right) \varphi = 0, \tag{72}$$

where the function $\varphi(y, z) = (2/\sqrt{3\sqrt{3}})\psi(y, z)$ is normalized to one, $\lambda = 4(E - \mathcal{E}_0 + 3J_0)/(3J_0)$ and $g_2 = 3\sqrt{3}\sigma/2$. Equation (72) always admits a delocalized solution while the localized self-trapped solutions, as was shown in [45] and [46], arise only when the nonlinearity constant g_2 exceeds the critical value $g_{2,\mathrm{cr}} = 2\pi$. From the definition of g_2 we derive the critical value σ_{cr}, which coincides with the one given in (69). The corresponding self-trapped state is characterized by the localization parameter and the energy

$$\kappa = \frac{1}{4}\sqrt{\frac{3\sqrt{3}(\sigma - \sigma_{\mathrm{cr},1})}{\pi\gamma}}, \qquad \mathcal{E}_{\mathrm{tot}}^{\mathrm{2D}} = \frac{3}{4} J_0 \left(\epsilon_0 - \frac{3\sqrt{3}(\sigma - \sigma_{\mathrm{cr},1})^2}{32\pi\gamma\sigma}\right), \tag{73}$$

respectively. To decide which type of solution is actually realized it is necessary to calculate the total energy of the system. In the continuum approximation with respect to the y and z coordinates this total energy, after the elimination of the phonon variables, is given by the expression

$$\mathcal{E}_{\mathrm{tot}} = \frac{3}{4} J_0 \int_{-3L/2}^{3L/2} \mathrm{d}z \int_0^{\sqrt{3}N} \mathrm{d}y$$

$$\times \left(\epsilon_0 |\varphi(y, z)|^2 + \left|\vec{\nabla}\varphi(y, z)\right|^2 - g_2 |\varphi(y, z)|^4 - \gamma g_2 \left(\vec{\nabla}|\varphi(y, z)|^2\right)^2\right), \tag{74}$$

where $\epsilon_0 = 4(\mathcal{E}_0 - 3J_0)/(3J_0)$.

Note that equation (72) possesses an azimuthally homogeneous solution of the form

$$\varphi(y, z) = \frac{1}{\sqrt{\sqrt{3}N}} \varphi(z). \tag{75}$$

Note also that after the rescaling which preserves the normalization condition, equation (72) again reduces to equation (42), which has been obtained in the approximation of one energy band and which possesses the solution (45). Substituting this solution into equation (74), we find the corresponding energy:

$$\mathcal{E}_{\mathrm{tot}}^{\mathrm{1D}} = \tfrac{3}{4} J_0 \left(\epsilon_0 - \epsilon_1\right), \qquad \epsilon_1 = \frac{3\sigma^2}{16N^2}, \tag{76}$$

which coincides with the energy of the azimuthally symmetric solution given by equations (52).

On the other hand, seeking a solution of the form

$$\varphi(y,z) = \varphi_0(z)\varphi_1(y), \tag{77}$$

where $\varphi_0(z)$ is given by (45) for a fixed value of $z = z_0$, we obtain from equation (72) the equation for $\varphi_1(y)$. The latter, after the rescaling $y = \sqrt{3}x/2$, $\varphi_1(y) = \sqrt{2/\sqrt{3}}\varphi(x)$, reduces to equation (63), which describes a separate zigzag chain in which the probability of a quasiparticle localization is maximal. The total energy of the system for the ansatz (77), (45), used as a trial function, is given by

$$\mathcal{E}_{\rm tot} = \frac{3}{4}J_0\int_0^{\sqrt{3}N} {\rm d}y\left((\epsilon_0+\epsilon_1)|\varphi(y)|^2 + \left|\frac{{\rm d}\varphi(y)}{{\rm d}y}\right|^2 - g_{\rm eff}|\varphi(y)|^4\right), \tag{78}$$

where

$$g_{\rm eff} = \frac{3\sqrt{3}\sigma^2}{8N}. \tag{79}$$

Note that we have written the energy expression (78), neglecting the term proportional to γ, since this term, in the 1D case, provides only a small correction, while its role in the 2D case is much more important since there it prevents the collapse of the self-trapped states.

The minimum energy condition for the functional (78) leads to an equation that coincides with equation (63) with the nonlinearity coefficient $g_{\rm eff}$ appearing instead of g_1. This equation always admits a homogenous solution $\varphi(x) = {\rm const} = 1/\sqrt{\sqrt{3}N}$ which corresponds to the eigenvalue and the total energy coinciding with the corresponding values of the azimuthally symmetric solution (given by equations (46) and (52)). As we have mentioned above, a solution with the broken azimuthal symmetry first arises when $g_{\rm eff}$ exceeds some critical value, namely, $g_{\rm eff} > g_{\rm eff,cr} = \pi^2/(\sqrt{3}N)$, which, therefore, gives the critical value of the coupling parameter σ:

$$\sigma_{\rm cr,2} = \frac{2\sqrt{2}\pi}{3} = 2.96. \tag{80}$$

The total energy of the system in this state is given by the expression

$$\mathcal{E}^{2D}_{\rm tot} = \frac{3}{4}J_0\left(\epsilon_0 - \left(\frac{3}{4}\right)^3\frac{\sigma^2}{\pi^2N^2}\left(\sigma^2 - \frac{4\pi^2}{9}\right)\right). \tag{81}$$

This energy, above the critical value $\sigma_{\rm cr,2}$, is lower than the energy of the 1D polaron (76).

6. Conclusion

Our analysis, performed in the adiabatic approximation, has shown that the self-trapping of quasiparticles can take place in a zigzag nanotube. We have shown that the corresponding system of equations admits several types of solution which possess different symmetries, and that the stability of these solutions depends on the strength of the electron–phonon coupling. Namely, as the coupling constant σ increases up to the lower critical value $\sigma_{\rm cr,1}$ at $\sigma < \sigma_{\rm cr,1}$, the quasiparticle becomes self-trapped in a quasi-1D polaron state. When σ increases further, i.e., at the intermediate values $\sigma_{\rm cr,1} < \sigma < \sigma_{\rm cr,2}$, the quasiparticle can be self-trapped in either a 2D azimuthally symmetrical polaron state or a 1D polaron state with a broken azimuthal symmetry. Finally, at $\sigma > \sigma_{\rm cr,2}$, it becomes an azimuthally nonsymmetrical small 2D polaron.

In general, our analytical results agree qualitatively and quantitatively with the numerical studies reported in [26]. These are summarized in figure 2 in the form of the phase diagram of the ground electron states in a zigzag nanotube depending on the dimensionless electron–phonon coupling, σ_0, and nanotube diameter, N. Here the solid lines correspond to the

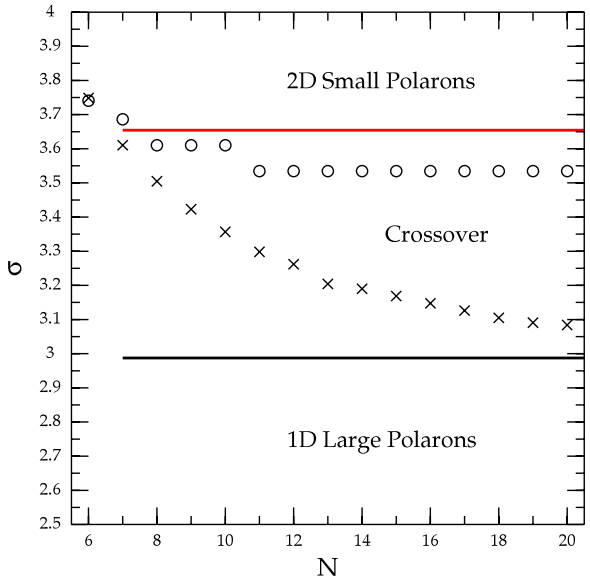

Figure 2. Domains of solutions, as a function of N, obtained in the numerical ($\chi_2/\sqrt{J_0 w} = 0.2$) and analytical studies. Above the top line (analytical) or circles (numerical): self-trapped 2D small polaron states. Below the bottom line (crosses): large polaron. Between the two regions, the crossover regime in which the two types of states coexist.

(This figure is in colour only in the electronic version)

analytical results, and the crosses and circles represent the numerical data. This diagram shows three regions of self-trapped electron states. In the region above the upper solid line an extra electron is self-trapped in a 2D small polaron state, below the lower solid line quasi-1D large polarons are formed, while in the region between these two solid lines the two types of state coexist. The corresponding three areas obtained numerically in [26] are separated by circles and crosses. The numerical results have been calculated for the coupling constant $\chi_2/\sqrt{J_0 w} = 0.2$ and $w_c/w = 0.2$; the analytical curves correspond to $p = 0.9$ (see equation (39)). Thus, our approximation $p \approx 1$, made above, is valid. The comparison of these results with what was seen in the numerical modelling justifies our analytical studies.

As we have shown in section 3, the Hamiltonian (10) effectively describes one extra electron in a half-filled band system with one electron per atom. Therefore, our model qualitatively describes self-trapped states of one or a few doped electrons in carbon nanotubes. Next, we have to estimate if the coupling constants for carbon nanotubes are below or above the corresponding critical values. The numerical value of the coupling constant σ_0,

$$\sigma_0 = \frac{(\chi_1 + J_1)^2}{J_0 w}, \tag{82}$$

can be estimated using the value for the radial force constant $w = 36.50 \times 10^4$ dyn cm^{-1} = 365 N m^{-1} (see [13]). A theoretical estimate of the hopping parameter $|J_0| = 2.5$ eV was obtained for 2D graphene which agrees with the experimental value $|J_0| = 2.7$ eV calculated to fit the scanning tunnelling microscopy (STM) density of states data [13, 47]. The parameter of electron–phonon interaction can be written as $J_1 = q_0 J_0$ (see [12]), where the coefficient $q_0 = 2.5$ Å^{-1} was calculated in [48]. Unfortunately, little is known about the constant χ_1. At $\chi_1 \neq 0$ the value of σ_0 can be either larger or smaller than the corresponding value at

$\chi_1 = 0$, $\sigma_0(\chi_1 = 0) \approx 0.6$–$0.7$, depending on the sign of χ_1. Nevertheless, in view of the significant difference between σ_0 and $\sigma_{\mathrm{cr},1} = 2.4$ we expect that, at low doping, extra electrons in carbon nanotubes are self-trapped in quasi-1D large polaron states. A detailed study of the electron–phonon interaction, using femtosecond time-resolved photoemission, has been performed in [49] by measuring the nonequilibrium electron dynamics after rapid heating of the system with a femtosecond laser pulse. This study has given the measured value of $q_0 \approx 1$ Å^{-1} which is considerably smaller than those derived in [48], i.e., a 50% discrepancy between the experimental and theoretical values. The same magnitude of the discrepancy for the values of the electron–phonon matrix elements has been obtained from the optical measurements [50] (11 meV) and *ab initio* calculations [51] (28 meV). Note, however, that in the long-wave limit from (88) we find that the electron–phonon matrix element $F_{\lambda,\lambda'}(k, \nu; q, \mu|\tau)$ is proportional to the sum $\chi_1 + J_1$, and, therefore, assuming that χ_1 and J_1 have opposite sign and setting $\chi_1 \approx -J_1/2$, the discrepancy between the experimental and theoretical values can be removed. For the experimental value of $q_0 \approx 1$Å^{-1} we obtain $\sigma_0 \approx 0.15$. Therefore, the quasi-1D large polaron is rather broad. As we have discussed above, such a polaron is stable in nanotubes of not too large diameters.

One can expect the manifestation of self-trapped polaron states in nanotubes to occur in their optical and transport properties. If the adiabatic approximation is valid, the scattering of solitons (large polarons) is determined by the residual electron–phonon interaction which can be regarded as a perturbation. In this case the scattering probability is small and, therefore, the dynamical properties of solitons provide a high mobility of the injected charge carriers leading to a ballistic transport. The residual scattering of solitons on phonons is important for a more accurate description of the transport and of the optical properties of the systems [41].

Acknowledgments

This work has been supported by a Royal Society grant. The authors LB and AE also acknowledge partial support from the Ukrainian State Granting Authority for Fundamental Research.

Appendix A. Lattice distortions and electron–phonon coupling functions

The deviations from the equilibrium values due to the lattice displacements $W_{æ,\delta(æ)} = \vec{r}_{æ,\delta(æ)} \cdot (\vec{U}_{\delta(æ)} - \vec{U}_{æ})$ are given by

$$\begin{aligned} W_{æ;r(æ)} &= \frac{\sqrt{3}}{2}\sin\left(\frac{\alpha}{4}\right)(u^1_{r(æ)} + u^1_{æ}) - (-1)^{\varrho}\frac{\sqrt{3}}{2}\cos\left(\frac{\alpha}{4}\right)(u^2_{r(æ)} - u^2_{æ}) \\ &\quad - \frac{(-1)^{\varrho}}{2}(u^3_{r(æ)} - u^3_{æ}), \\ W_{æ;l(æ)} &= \frac{\sqrt{3}}{2}\sin\left(\frac{\alpha}{4}\right)(u^1_{l(æ)} + u^1_{æ}) + (-1)^{\varrho}\frac{\sqrt{3}}{2}\cos\left(\frac{\alpha}{4}\right)(u^2_{l(æ)} - u^2_{æ}) \\ &\quad - \frac{(-1)^{\varrho}}{2}(u^3_{l(æ)} - u^3_{æ}), \\ W_{æ;d(æ)} &= (-1)^{\varrho}(u^3_{d(æ)} - u^3_{æ}). \end{aligned} \tag{83}$$

For the deviation of the solid angle spanned by the three lattice vectors, located at a given site, from the equilibrium value due to site displacements, we have

$$C_{æ} = \frac{\sqrt{3}}{2}\Bigg[3\cos^3\left(\frac{\alpha}{4}\right)u^1_{æ} - \cos\left(\frac{\alpha}{4}\right)u^1_{d(æ)} - \cos\left(\frac{\alpha}{4}\right)\left(\frac{5}{2}\cos^2\left(\frac{\alpha}{4}\right) - \frac{3}{2}\right)(u^1_{l(æ)} + u^1_{r(æ)})$$
$$+ (-1)^{\varrho}\sin\left(\frac{\alpha}{4}\right)\left(\frac{3}{2} - \frac{5}{2}\sin^2\left(\frac{\alpha}{4}\right)\right)(u^2_{l(æ)} - u^2_{r(æ)})$$
$$+ (-1)^{\varrho}\frac{\sqrt{3}}{4}\sin\left(\frac{\alpha}{2}\right)(u^3_{l(æ)} + u^3_{r(æ)} - 2u^3_{æ})\Bigg]. \tag{84}$$

The shift deformation, due to the site displacements, defined as $\Omega_{æ;r(æ)} = \vec{r}^{\perp}_{æ,\delta(æ)} \cdot (\vec{U}_{\delta(æ)} - \vec{U}_{æ})$, is given by

$$\Omega_{æ;r(æ)} = -\Bigg[\frac{1}{2}\sin\left(\frac{\alpha}{4}\right)(u^1_{r(æ)} + u^1_{æ}) - \frac{(-1)^{\varrho}}{2}\cos\left(\frac{\alpha}{4}\right)(u^2_{r(æ)} - u^2_{æ})$$
$$+ \frac{(-1)^{\varrho}\sqrt{3}}{2}(u^3_{r(æ)} - u^3_{æ})\Bigg], \tag{85}$$
$$\Omega_{æ;l(æ)} = \frac{1}{2}\sin\left(\frac{\alpha}{4}\right)(u^1_{l(æ)} + u^1_{æ}) + \frac{(-1)^{\varrho}}{2}\cos\left(\frac{\alpha}{4}\right)(u^2_{l(æ)} - u^2_{æ}) + \frac{(-1)^{\varrho}\sqrt{3}}{2}(u^3_{l(æ)} - u^3_{æ}),$$
$$\Omega_{æ;d(æ)} = -(-1)^{\varrho}(u^2_{d(æ)} - u^2_{æ}).$$

The matrix of the unitary transformation coefficients $\|v_{\varrho,\lambda}(k,\nu)\|$, defined in (12), is given by

$$\|v_{\varrho,\lambda}(k,\nu)\| = \left\| \begin{matrix} e^{-i(\frac{k+\nu}{4}+\theta^{(0)}_{+})} & e^{-i(\frac{k+\nu}{4}-\theta^{(0)}_{-})} & e^{-i(\frac{k+\nu}{4}-\theta^{(0)}_{-})} & e^{-i(\frac{k+\nu}{4}+\theta^{(0)}_{+})} \\ e^{-i(\frac{k-\nu}{4}-\theta^{(0)}_{+})} & e^{-i(\frac{k-\nu}{4}+\theta^{(0)}_{-})} & -e^{-i(\frac{k-\nu}{4}+\theta^{(0)}_{-})} & -e^{-i(\frac{k-\nu}{4}-\theta^{(0)}_{+})} \\ e^{i(\frac{k+\nu}{4}-\theta^{(0)}_{+})} & -e^{i(\frac{k+\nu}{4}+\theta^{(0)}_{-})} & -e^{i(\frac{k+\nu}{4}+\theta^{(0)}_{-})} & e^{i(\frac{k+\nu}{4}-\theta^{(0)}_{+})} \\ e^{i(\frac{k-\nu}{4}+\theta^{(0)}_{+})} & -e^{i(\frac{k-\nu}{4}-\theta^{(0)}_{-})} & e^{i(\frac{k-\nu}{4}-\theta^{(0)}_{-})} & -e^{i(\frac{k-\nu}{4}+\theta^{(0)}_{+})} \end{matrix} \right\|, \tag{86}$$

where the phases $\theta^{(0)}_{\pm} = \theta^{(0)}_{\pm}(k,\nu)$ are determined from the relations

$$\tan 2\theta^{(0)}_{\pm}(k,\nu) = \frac{\sin\frac{k}{2}}{2\cos\frac{\nu}{2} \pm \cos\frac{k}{2}}. \tag{87}$$

Finally, the function of the electron–phonon coupling, introduced in (10), is given by the expression

$$F_{\lambda,\lambda'}(k,\nu;q,\mu|\tau) = \frac{1}{4\sqrt{M}}\sum_{\varrho}\Big[\chi_1\sum_{\delta}W_{\varrho,\delta}(q,\mu,\tau) + \chi_2 C_{\varrho,\tau}(q,\mu)\Big]$$
$$\times v^*_{\varrho,\lambda}(k,\nu)v_{\varrho,\lambda'}(k-q,\nu-\mu)$$
$$+ \frac{J_1}{4\sqrt{M}}\Big[\Big(W_{1,r}(q,\mu,\tau) + e^{-i(\nu-\mu)}W_{1,l}(q,\mu,\tau)\Big)$$
$$\times v^*_{1,\lambda}(k,\nu)v_{2,\lambda'}(k-q,\nu-\mu)$$
$$+ \Big(W_{2,r}(q,\mu,\tau) + e^{i(\nu-\mu)}W_{2,l}(q,\mu,\tau)\Big)v^*_{2,\lambda}(k,\nu)v_{1,\lambda'}(k-q,\nu-\mu)$$
$$+ e^{-i(k-q)}W_{1,d}(q,\mu,\tau)v^*_{1,\lambda}(k,\nu)v_{4,\lambda'}(k-q,\nu-\mu)$$
$$+ e^{i(k-q)}W_{4,d}(q,\mu,\tau)v^*_{4,\lambda}(k,\nu)v_{1,\lambda'}(k-q,\nu-\mu)$$
$$+ W_{2,d}(q,\mu,\tau)v^*_{2,\lambda}(k,\nu)v_{3,\lambda'}(k-q,\nu-\mu)$$
$$+ W_{3,d}(q,\mu,\tau)v^*_{3,\lambda}(k,\nu)v_{2,\lambda'}(k-q,\nu-\mu)$$
$$+ \Big(e^{i(\nu-\mu)}W_{3,r}(q,\mu,\tau) + W_{3,l}(q,\mu,\tau)\Big)v^*_{3,\lambda}(k,\nu)v_{4,\lambda'}(k-q,\nu-\mu)$$
$$+ \Big(e^{-i(\nu-\mu)}W_{4,r}(q,\mu,\tau) + W_{4,l}(q,\mu,\tau)\Big)v^*_{4,\lambda}(k,\nu)v_{3,\lambda'}(k-q,\nu-\mu)\Big]. \tag{88}$$

Appendix B. The Hubbard model

The Hubbard model [52] is one of the few realistic models which takes into consideration the electron correlation in a discrete lattice and which is hopefully amenable to mathematical treatment [52–55]. The 1D model with the short-range electron–electron interaction in the one-band approximation has been solved exactly and completely by means of the Bethe functions (the Bethe ansatz) [53]. The Hubbard Hamiltonian, $H_{\rm H} = H_0 + H_{\rm e-e}$, involves the electron hopping between neighbouring lattice sites

$$H_0 = \sum_{n,\sigma}\left[\mathcal{E}_0\, a^{\dagger}_{n,\sigma}a_{n,\sigma} - J_0\left(a^{\dagger}_{n,\sigma}a_{n+1,\sigma} + a^{\dagger}_{n+1,\sigma}a_{n,\sigma}\right)\right], \tag{89}$$

and the Coulomb repulsion between electrons at each site which is capable of accommodating two electrons of opposite spins,

$$H_{\rm e-e} = \tfrac{1}{2}V_0\sum_{n,\sigma} n_{n,\sigma}n_{n,\bar{\sigma}}. \tag{90}$$

Here J_0 is the energy of the electron hopping interaction between sites, $V_0 > 0$ is the on-site energy of the electron–electron Coulomb repulsion, $n_{n,\sigma} = a^{\dagger}_{n,\sigma}a_{n,\sigma}$, and $\bar{\sigma} = -\sigma$. In (89), $\mathcal{E}_0$ is the energy of a bound electron level on a site $\mathcal{E}_0 = -E_0$, counting the energy from the continuum states of free electrons. The Hamiltonian preserves the total number of electrons $N_{\rm e} = \sum_{n,\sigma} a^{\dagger}_{n,\sigma}a_{n,\sigma}$ and the total spin $S = \sum_{n,\sigma}\sigma a^{\dagger}_{n,\sigma}a_{n,\sigma}$.

Next we consider exact solutions of the Schrödinger equation

$$H_{\rm H}|\Psi\rangle = E|\Psi\rangle \tag{91}$$

for the 1D Hubbard model using the η-pairing approach developed by Yang [54]. Note that this approach goes beyond the 1D case. It is applicable to 2D and 3D lattices and can be generalized to the carbon nanotube geometry. Here we consider, for simplicity, the 1D case. As is shown in [54], many eigenstates of equation (91) can be explicitly written down with the aid of an operator η defined as

$$\eta = \sum_n {\rm e}^{-{\rm i}\pi n}a_{n,\sigma}a_{n,\bar{\sigma}}. \tag{92}$$

The state

$$|\Psi_M\rangle = A_M\left(\eta^{\dagger}\right)^M|0\rangle, \tag{93}$$

with A_M being a normalization factor, is an eigenstate of the Hamiltonian $H_{\rm H}$ with the eigenvalue

$$E_M = M\left(2\mathcal{E}_0 + V_0\right). \tag{94}$$

The state (93) is one of many possible electron states, but not the ground state, with $S = 0$ in a lattice with $N_{\rm e} = 2M$ electrons. In the case of a half-filled band $M = N/2$ (N, assumed to be even, is the number of lattice sites in the main region).

Using the η-operator, we can also construct the state

$$|\Psi_{\rm e}\rangle = \sum_n \psi_n a^{\dagger}_{n,\sigma}\left(\eta^{\dagger}\right)^{N/2}|0\rangle, \tag{95}$$

which corresponds to an extra electron in a half-filled-band lattice. One can easily verify that such states are eigenstates of equation (91) provided that $\psi_n = B\exp({\rm i}kn)$ (B is a normalization factor). The corresponding energies of these states are

$$E_{\rm e} = E_{\rm e}(k) = (N+1)\mathcal{E}_0 + \frac{N}{2}V_0 - 2J_0\cos k, \tag{96}$$

where $k = 2\pi\nu/N$, $\nu = 0, \pm1, \ldots, \pm((N/2) - 1), N/2$. Here we assume that the chain is long enough, $N \gg 1$, and apply periodic boundary conditions. Therefore, an extra electron in a half-filled-band lattice can be effectively described by H_0, which gives the same dispersion law as (96).

References

[1] Froehlich H 1952 *Proc. R. Soc.* A **215** 291
[2] Peierls R E 1955 *Quantum Theory of Solids* (Oxford: Clarendon)
[3] Su W P, Schriefer J R and Heeger A J 1970 *Phys. Rev. Lett.* **42** 1698
Su W P, Schriefer J R and Heeger A J 1980 *Phys. Rev.* B **22** 2099
[4] Davydov A S 1985 *Solitons in Molecular Systems* (Dordrecht: Reidel)
[5] Holstein T 1959 *Ann. Phys.* **8** 325
[6] Rashba E I 1957 *Izv. Akad. Nauk. UkrSSR, ser. Fiz.* **21** 37 (in Russian)
Rashba E I 1958 *Opt. Spektrosk.* **2** 75 (in Russian)
Rashba E I 1958 *Opt. Spektrosk.* **2** 88 (in Russian)
[7] Conwell E M and Rakhmanova S V 2000 *Proc. Natl Acad. Sci. USA* **97** 4556
[8] Wilson E G 1983 *J. Phys. C: Solid State Phys.* **16** 6739
[9] Heeger A J, Kivelson S, Schrieffer J R and Su W-P 1988 *Rev. Mod. Phys.* **60** 781
[10] Rice M J and Phillpot S R 1987 *Phys. Rev. Lett.* **58** 937
[11] Rice M J, Phillpot S R, Bishop A R and Campbell D K 1986 *Phys. Rev.* B **34** 4139
[12] Jishi R A, Dresselhaus M S and Dresselhaus G 1993 *Phys. Rev.* B **48** 11385
[13] Saito R, Dresselhaus G and Dresselhaus M S 1998 *Physical Properties of Carbon Nanotubes* (London: Imperial College Press)
[14] Dresselhaus M S, Dresselhaus G and Ekland P C 1996 *Science of Fullerens and Carbon Nanotubes* (New York: Academic)
[15] Dai H 2002 *Surf. Sci.* **500** 208
[16] Chopra N G *et al* 1995 *Science* **269** 966
[17] Hemraj-Benny T *et al* 2005 *Phys. Chem. Chem. Phys.* **7** 1103
[18] Mintmire J W, Dunlap B I and White C T 1992 *Phys. Rev. Lett.* **68** 631
[19] Kane C L and Mele E J 1997 *Phys. Rev. Lett.* **78** 1932
[20] Verissimo-Alves M, Capaz R B, Koiller B, Artacho E and Chacham H 2001 *Phys. Rev. Lett.* **86** 3372
[21] Prylutskyy Yu, Suprun A and Ogloblya O 2002 *Int. Conf. on Theoretical Physics (Paris, UNESCO, July 2002)* p 278 (Book of abstracts)
Prylutskyy Yu I, Ogloblya O V, Eklund P and Scharff P 2001 *Synth. Met.* **121** 1209–10
[22] Hirori H, Matsuda K, Miyauchi Y, Maruyama S and Kanemitsu Y 2006 *Phys. Rev. Lett.* **97** 257401
[23] Brizhik L S, Eremko A A, Piette B and Zakrzewski W J 2004 *Phys. Rev.* E **70** 031914
[24] Saito R, Fujita M, Dresselhaus G and Dresselhaus M S 1992 *Appl. Phys. Lett.* **60** 2204
[25] Duclaux L 2002 *Carbon* **40** 1751
[26] Bratek L, Brizhik L, Eremko A, Piette B, Watson M and Zakrzewski W 2007 *Physica* D **228** 130
[27] Mahan G D 2003 *Phys. Rev.* B **68** 125409
[28] Hamada N, Sawada S and Oshiyama A 1992 *Phys. Rev. Lett.* **68** 1579
[29] Saito R, Fujita M, Dresselhaus G and Dresselhaus M S 1992 *Phys. Rev.* B **46** 1804
Saito R, Fujita M, Dresselhaus G and Dresselhaus M S 1992 *Appl. Phys. Lett.* **60** 2204
[30] Dresselhaus M S, Dresselhaus G and Saito R 1992 *Phys. Rev.* B **45** 6234
[31] Woods L M and Mahan G D 2000 *Phys. Rev.* B **61** 10651
[32] Saito R and Kamimura H 1983 *J. Phys. Soc. Japan* **52** 407
[33] Suzuura H and Ando T 2002 *Phys. Rev.* B **65** 235412
[34] Jiang J, Saito R, Gruneis A, Chou S G, Samsonidze Ge G, Jorio A, Dresselhaus G and Dresselhaus M S 2005 *Phys. Rev.* B **71** 205420
Jiang J, Saito R, Gruneis A, Chou S G, Samsonidze Ge G, Jorio A, Dresselhaus G and Dresselhaus M S 2005 *Phys. Rev.* B **71** 045417
[35] Jiang J, Saito R, Gruneis A, Dresselhaus G and Dresselhaus M S 2004 *Chem. Phys. Lett.* **392** 383
[36] Egger R and Gogolin A O 1997 Effective low-energy theory for correlated carbon nanotubes *Phys. Rev. Lett.* **79** 5082–5
[37] Krotov Yu A, Lee D-H and Louie S 1997 *Phys. Rev. Lett.* **78** 4245
[38] Balents L and Fisher M P A 1997 *Phys. Rev.* B **55** R11973–6

[39] Tang Z K, Zhang L, Wang N, Zhang X X, Wen G H, Li G D, Wang J N, Chan C T and Sheng P 2001 *Science* **292** 2467
[40] Thess A *et al* 1996 *Science* **273** 483
Fisher J E *et al* 1997 *Phys. Rev.* B **55** R4921
[41] De Filippis G, Cataudella V, Mishchenko A S, Perroni C A and Devreese J T 2006 *Phys. Rev. Lett.* **96** 136405
[42] Fomin V M, Gladilin V N, Devreese J T, Pokatilov E P, Balaban S N and Klimin S N 1998 *Phys. Rev.* B **57** 2415
[43] Brizhik L S, Eremko A A, Piette B and Zakrzewski W 2006 *Physica* D **218** 36
[44] Bateman H and Erdelyi A 1955 *Higher Transcendental Functions* vol 3 (New York: Mc-Graw Hill)
[45] Brizhik L S, Eremko A A, Piette B and Zakrzewski W J 2003 *J. Math. Phys.* **44** 3689
[46] Brizhik L S, Eremko A A, Piette B and Zakrzewski W J 2003 *Nonlinearity* **16** 1481
[47] Mintmire J W and White C T 1995 *Carbon* **33** 893
Wildöer J W G, Venema L C, Rinzler A G, Smally R E and Dekker C 1998 *Nature* **391** 59–62
[48] Pietronero L, Strässler S, Zeller H R and Rice M J 1980 *Phys. Rev.* B **22** 904
[49] Hertel T and Moos G 2000 *Phys. Rev. Lett.* **84** 5002–5
[50] Yin Y, Vamivokas A, Walsh A, Cronin S, Ünlü M S, Goldberg B B and Swan A K 2006 *Preprint* cond-mat/0605670
[51] Machón M, Reich S, Telg H, Maultzsch J, Ordejón P and Thomsen C 2005 *Phys. Rev.* B **71** 035416
[52] Hubbard J 1963 *Proc. R. Soc.* **276** 238
Hubbard J 1964 *Proc. R. Soc.* **277** 237
[53] Lieb E H and Wu F Y 1968 *Phys. Rev. Lett.* **20** 1445
[54] Yang C N 1989 *Phys. Rev. Lett.* **63** 2144
[55] Lee D 2006 *Phys. Rev.* B **73** 115112